

## BAYESIAN META-ANALYSIS FOR IDENTIFYING PERIODICALLY EXPRESSED GENES IN FISSION YEAST CELL CYCLE<sup>1</sup>

BY XIAODAN FAN, SAUMYADIPTA PYNE AND JUN S. LIU

*Harvard University and Chinese University of Hong Kong, Broad Institute and Harvard University*

The effort to identify genes with periodic expression during the cell cycle from genome-wide microarray time series data has been ongoing for a decade. However, the lack of rigorous modeling of periodic expression as well as the lack of a comprehensive model for integrating information across genes and experiments has impaired the effort for the accurate identification of periodically expressed genes. To address the problem, we introduce a Bayesian model to integrate multiple independent microarray data sets from three recent genome-wide cell cycle studies on fission yeast. A hierarchical model was used for data integration. In order to facilitate an efficient Monte Carlo sampling from the joint posterior distribution, we develop a novel Metropolis–Hastings group move. A surprising finding from our integrated analysis is that more than 40% of the genes in fission yeast are significantly periodically expressed, greatly enhancing the reported 10–15% of the genes in the current literature. It calls for a reconsideration of the periodically expressed gene detection problem.

**1. Introduction.** The cell division cycle is the concerted sequence of processes by which a cell duplicates its DNA and divides into two daughter cells. Many genes are expressed periodically at a specific stage during the cell cycle when they peak and trough over a certain time range. They are termed as “cell cycle-regulated genes.” Here, in the context of mRNA expression studies, we call these “Periodically Expressed (PE) genes.” In contrast, other genes are called “Aperiodically Expressed (APE) genes.” Identification of PE genes is both of theoretical importance because of the need to understand the different mechanisms underlying these genes’ involvements

---

Received January 2009; revised September 2009.

<sup>1</sup>Supported in part by the NIH Grant R01GM078990 and the NSF Grant DMS-07-06989.

*Key words and phrases.* Cell cycle, periodically expressed gene, microarray time series, meta-analysis, fission yeast, *Schizosaccharomyces pombe*, Markov chain Monte Carlo.

<p>This is an electronic reprint of the original article published by the <a href="#">Institute of Mathematical Statistics</a> in <i>The Annals of Applied Statistics</i>, 2010, Vol. 4, No. 2, 988–1013. This reprint differs from the original in pagination and typographic detail.</p>
--

in the cell cycle processes, and of practical importance due to the biological links between cell cycle control and many diseases such as cancer [Sherr (1996); Whitfield et al. (2002); Bar-Joseph et al. (2008)].

With the help of the microarray techniques and various cell phase synchronization methods (synchronizing the progression of cells through the stages of cell cycle), researchers have conducted genome-wide time series expression analyses on synchronized cells for various species ranging from fungi to plant to human [Cho et al. (1998); Spellman et al. (1998); Laub et al. (2000); Ishida et al. (2001); Menges et al. (2002); Whitfield et al. (2002); Rustici et al. (2004); Oliva et al. (2005); Peng et al. (2005); Bar-Joseph et al. (2008)]. Several strategies for identifying PE genes on these data have been developed, such as the fitting of a sinusoidal function [Spellman et al. (1998)], clustering techniques [Eisen et al. (1998); Whitfield et al. (2002)], the single-pulse model [Zhao, Prentice and Breeden (2001)], the partial least squares regression approach [Johansson, Lindgren and Berglund (2003)], the average periodogram [Wichert, Fokianos and Strimmer (2004)], the linear combination of cubic  $B$ -spline basis [Luan and Li (2004)], the random-periods model [Liu et al. (2004)], the least square fitting for the periodic-normal mixture model [Lu et al. (2004)], the Fourier score combined with  $p$ -value of regulation [de Lichtenberg et al. (2005)], the robust spectral estimator combined with  $g$ -statistic [Ahdesmaki et al. (2005)] and the up-down signature method [Willbrand et al. (2005)]. Zhou, Wakefield and Breeden (2005) applied a Bayesian approach for single experiment data by fixing the period at pre-estimated value. Most of these methods use a set of known PE genes to estimate the cell cycle period prior to testing the periodicity for other genes.

While the previous efforts have often reported positively about the presence of the periodic signal in these gene expression data, doubts were raised as to whether such periodic gene regulation was reproducible [Shedden and Cooper (2002); Wichert, Fokianos and Strimmer (2004)] and, by extension, about the identity and count of PE genes discovered by subsequent analyses. One prevalent reason for skepticism is the reliance of many of the studies on ad hoc thresholds to classify genes as PE or otherwise. For example, Cho et al. (1998) detected the PE genes by visual inspection; Spellman et al. (1998) designed a cutoff value based on prior biological knowledge. Another possible reason is that the commonly assumed white noise background model for time series might be too unrealistic to allow correct inference about the identity and count of PE genes [Futschik and Herzel (2008)]. Furthermore, all previous approaches were designed for analyzing single time series per gene, which did not allow for an efficient combination of data from multiple experiments and therefore lacked the power to identify a large fraction of all PE genes. Recently Tsiporkova and Boeva (2008) proposed a procedure to combine multi-experiment data based on a dynamic time warping alignment

technique, which is potentially useful for analyzing multiple cell cycle data sets if combined with a periodicity detection algorithm. However, the procedure requires each time point within a time series to be aligned to a time point within the other time series, which is not always appropriate when the lengths of cell cycle period, the sampled time ranges and the sampling frequencies are all different between experiments.

Recently, three independent studies [Rustici et al. (2004); Oliva et al. (2005); Peng et al. (2005)] conducted elutriation and *cdc25* block-release synchronization experiments to measure genome-wide expression in the fission yeast (*Schizosaccharomyces pombe*) cell cycle. The results from these three studies also showed discrepancies with regard to the identity and count of PE genes. They reported 407, 747 and 750 PE genes, respectively, with only 176 genes being common to all three lists. However, the availability of 10 genome-wide experiments produced by these three different labs has made the fission yeast currently the organism with the largest cell cycle transcriptome data, which provides us an opportunity to obtain a better understanding of the cell cycle. Marguerat et al. (2006) combined the ten data sets from the three studies by multiplying  $p$ -values for gene regulation and periodicity from each experiment. They concluded that no more than about 500 PE genes can be reliably identified from the combined data. While observing that well over 1000 fission yeast genes could be periodically expressed and that each study had detected a different subset of these, they attributed the discrepancy to inconsistent gene naming, the use of different data analysis methods and the use of arbitrary thresholds.

We investigated the PE gene identification problem by employing a Bayesian approach to provide (1) a more realistic and comprehensive model for the cell cycle time series data, and (2) an efficient and rigorous way to combine data from multiple experiments. A hierarchical model together with MCMC computation is used to integrate different sources of variation and correlation into a single coherent probabilistic framework. We applied this approach to integrate the ten genome-wide time series data sets. A striking finding from our analysis is that more than 2000 genes are significantly periodically expressed. This number greatly enhances the count of possible cell cycle regulated genes in the current literature. Most interestingly, our finding can be visualized clearly from Figure 3, which merely displays the *original* data, but with the genes ordered according to our inferred periodicity strength and peaking phase.

**2. Materials and methods.** In Section 2.1 we describe the cell cycle gene expression data. In Section 2.2 we outline our parametric model for cell cycle gene expression. The Bayesian computation of the model is described in Section 2.3 and Section 2.4. In Section 2.5 we present our strategies for distinguishing PE genes from APE genes based on the model fitting results.

TABLE 1  
*Summary of the ten experiments for the fission yeast cell cycle*

Data set name	Rustici et al.					Peng et al.		Oliva et al.		
Microarray type	spotted PCR array					spotted oligo array		spotted PCR array		
Synchronization technique	elutriation			cdc25		elutriation	cdc25	elutriation		cdc25
Experiment name	Exp1	Exp2	Exp3	Exp4	Exp5	Exp6	Exp7	Exp8	Exp9	Exp10
Number of covered gene	4113	3921	4176	4281	4173	4263	4571	4543	4400	4727
Number of time point ( $S_e$ )	20	20	20	19	18	33	38	33	50	52
Time point frequency (min)	15	15	15	15	15	10	10	15–21	2–10	10–15

*Note:*

1. The data set Rustici et al. is downloaded from [http://www.sanger.ac.uk/PostGenomics/S\\_pombe/projects/cellcycle/](http://www.sanger.ac.uk/PostGenomics/S_pombe/projects/cellcycle/). Peng et al. is downloaded from [http://giscompute.gis.a-star.edu.sg/~gisljh/CDC/CDC\\_dnld\\_data.html](http://giscompute.gis.a-star.edu.sg/~gisljh/CDC/CDC_dnld_data.html). Oliva et al. is downloaded from [http://publications.redgreengene.com/oliva\\_plos\\_2005/](http://publications.redgreengene.com/oliva_plos_2005/).

2. The downloaded data set Rustici et al. has been normalized on an array-by-array basis using an in-house normalization script, which performs three steps: masking bad spots, filtering lower quality spots, applying local window-based normalization. Peng et al. has filtered low intensity features (2-fold less than the background) and done LOWESS normalization within array. Oliva et al. has been normalized within array by the GenePix Pro software with default setting.

3. Elutriation experiments are done to wild-type fission yeast, where samples of uniformly sized cells are obtained. Because cell size is correlated with cell cycle stage, these cells are synchronized with respect to their position in the cycle. Cdc25 block-and-release experiments are done to the fission yeast strain carrying the temperature-sensitive cdc25-22 mutant gene, where cells are initially synchronized by blocking them at some particular cell cycle stage, then releasing them from the block and taking samples at different times.

2.1. *Microarray time series data.* We obtained the normalized gene expression data for ten genome-wide experiments by three cell cycle microarray studies [Rustici et al. (2004); Oliva et al. (2005); Peng et al. (2005)] from the websites listed in Table 1. For each experiment, a culture of cells is grown and synchronized. A set of microarrays is used to measure gene expressions at selected time points (possibly with technical replication of the microarray). All values were converted to log-ratios with base 2. To make the log-ratios comparable across arrays, we transformed the values for every array separately to set the median log-ratio of each array to zero. Log-ratios from technical replicates, if present, were averaged. Time series with more than 25 percent missing entries were omitted. We unified gene names across the studies based on GeneDB database entries [Hertz-Fowler et al. (2004)]. The genes without a consistent nomenclature were excluded.

Let  $Y_{get}$  denote the gene expression log-ratio at time  $T_{et}$  in experiment  $e$  for gene  $g$ , where  $g = 1, \dots, G$ ,  $e = 1, \dots, E$ ,  $t = 1, \dots, S_e$ . Here  $Y_{get}$  is the observed data;  $T_{et}$ , the time of the measurement;  $G$ , the total number of genes studied;  $E$ , the total number of independent experiments; and  $S_e$ , the total number of time points measured in experiment  $e$ . The whole data set can be visualized as a G-by-E matrix of time series, where each row corresponds to one gene and each column corresponds to one experiment. If we pool together all filtered data from the ten data sets, we have that  $G = 4994$ ,  $E = 10$ , and  $S_e$  ranges from 18 to 52. A detailed overview of the data is given in Table 1. For illustration, the data for two genes are shown in Figure 1.

2.2. *Model.* We model each time series as a mean curve with additive independent and identically distributed (i.i.d.) Gaussian noise for measured time points. The mean curve is a function of time consisting of a trend component and a periodic component. For the trend component, we use a linear function along with a truncated quadratic function to model the block-release effect [artifacts introduced by experimental protocols for synchronization; see Lu et al. (2004)] and the general trend shown by the time series. We assume a first order Fourier model for the periodic component. A damping term is added to the periodic component to model the cell cycle de-synchronization effect, which implies that the periodic phenomenon eventually disappears as time increases. To model the whole matrix of time series, we assume that the periodic components for all genes within one experiment share the same period, which is equal to the cell division time (i.e., duration between the birth of a cell up to its division into two daughter cells). We further assume that the relative peak time within the cell cycle for every gene is fixed, which allows all genes to share the same phase shift when the periodic components across experiments are compared. More specifically, we

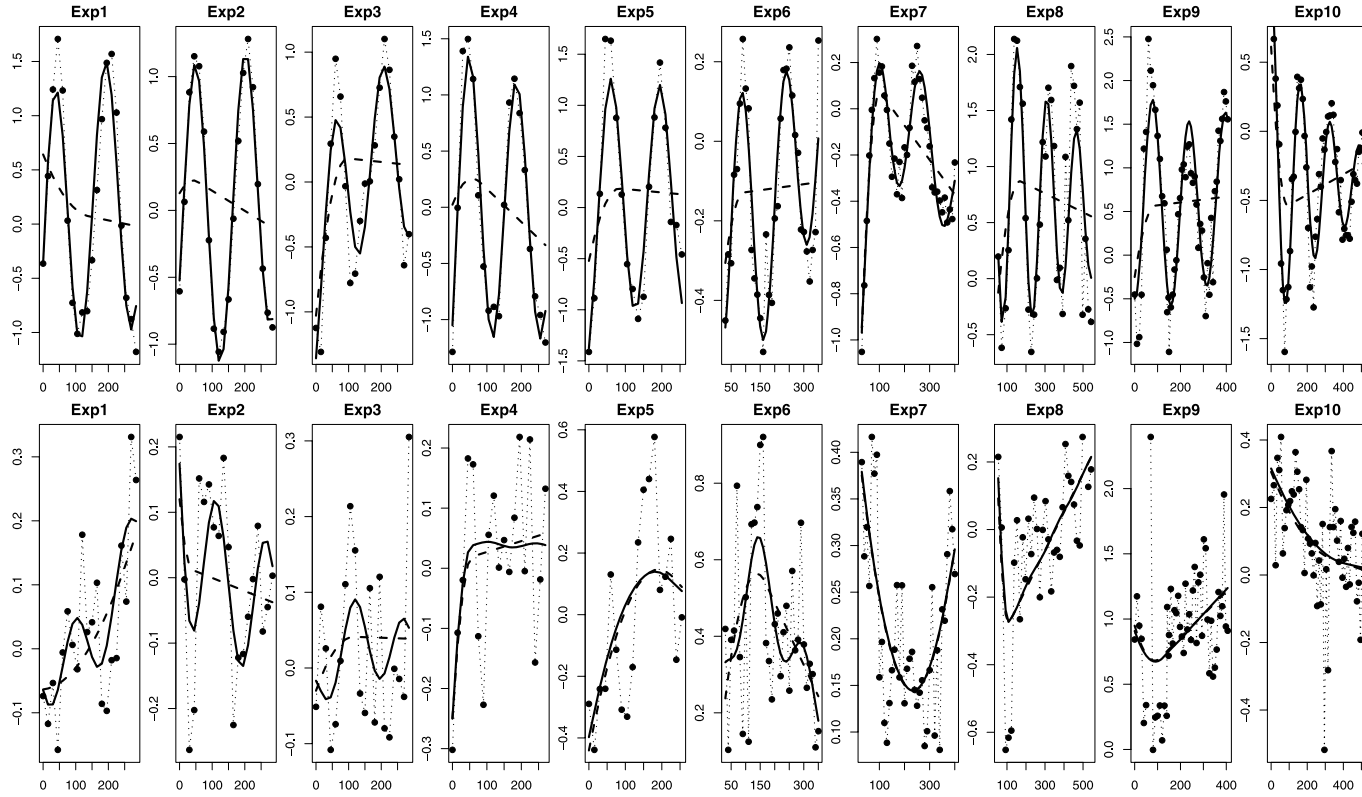


FIG. 1. Observed data and fitted mean curves for two samples of genes. For each sub-figure, the horizontal axis is the time (minutes) and the vertical axis is the gene expression value (log-ratio). The first row of sub-figures shows the ten time series for a known PE gene (*SPAPYUG7.03C*). The second row is for a stress response gene (*SPAC23C4.09C*), which is not regulated by the cell cycle. The bullet dots are the observed data. They are connected by dotted lines. The solid lines are the mean curves obtained by fitting the  $M_1$  model to the data. The dashed lines are the mean curves obtained by fitting the  $M_0$  model to the data. The details of model fitting are given in the following text.

assume the following model ( $M_1$ ) for each time series:

$$Y_{get} = a_{ge} + b_{ge}T_{et} + c_{ge}(\min(T_{et} - d_{ge}, 0))^2 + A_{ge} \cos(\mu_e T_{et} + \psi_e + \phi_g)e^{-\lambda_e T_{et}} + \varepsilon_{get},$$

where

- $a_{ge} + b_{ge}T_{et} + c_{ge}(\min(T_{et} - d_{ge}, 0))^2$ : trend component,
- $A_{ge} \cos(\mu_e T_{et} + \psi_e + \phi_g)e^{-\lambda_e T_{et}}$ : periodic component,
- $\varepsilon_{get} \sim N(0, \sigma_{ge}^2)$ : i.i.d. noise,
- $a_{ge}, b_{ge}$ : coefficients of the linear trend of a time series,
- $d_{ge}$ : ending time of block-release effect of a time series,
- $c_{ge}$ : magnitude of block-release effect of a time series,
- $\sigma_{ge}^2$ : noise level of a time series,
- $A_{ge}$ : amplitude of periodic component of a time series,
- $\mu_e$ : cell cycle angular frequency, equal to  $2\pi$  divided by the period of cell cycle of an experiment,
- $\psi_e$ : experiment-specific phase, which models the phase-shift between two experiments,
- $\phi_g$ : gene-specific phase, which decides its peaking time,
- $\lambda_e$ : magnitude of the de-synchronization effect of an experiment.

For each gene, we use different amplitude parameter  $A_{ge}$  for different experiments to account for the effects of different experimental platforms and synchronization techniques. If a gene is not periodic, the fitted amplitude  $A_{ge}$  should be close to zero. For such time series, the phase parameter  $\phi_g$  is redundant. To capture different noise levels in different experiments, we specify a hierarchical structure for the noise component by assuming that all  $\sigma_{ge}^2$  from the same experiment share the same inverse chi-square distribution with chosen degree of freedom  $C_{12}$  (a constant specified in the [Appendix](#)) and unknown hyper-parameters  $\zeta_e$ :

$$\sigma_{ge}^2 | \zeta_e \sim \text{Inv-}\chi^2(C_{12}, \zeta_e).$$

For convenience, we introduce the following notation:

- $Y \equiv \{Y_{get}, \text{ for } g = 1, \dots, G; e = 1, \dots, E; t = 1, \dots, S_e\}$ : expression values,
- $\Theta_e \equiv \{\mu_e, \psi_e, \lambda_e, \zeta_e\}$ : experiment-specific parameters,
- $\Theta \equiv \{\Theta_1, \dots, \Theta_E\}$ ,
- $\Phi \equiv \{\phi_1, \dots, \phi_G\}$ : gene phases,
- $\Gamma_{ge} \equiv \{a_{ge}, b_{ge}, c_{ge}, d_{ge}, A_{ge}, \sigma_{ge}^2\}$ : time-series-specific parameters,
- $\Gamma_g \equiv \{\Gamma_{g1}, \dots, \Gamma_{gE}\}$ ,
- $\Gamma \equiv \{\Gamma_1, \dots, \Gamma_G\}$ .

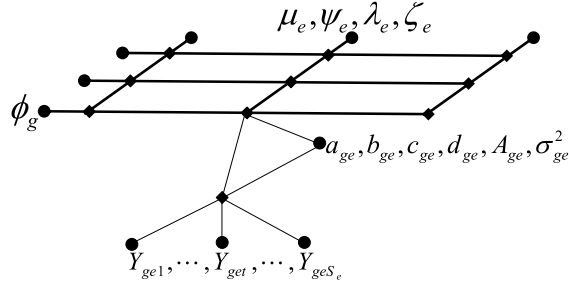


FIG. 2. *Dependence structure of all variables. All links are undirected. Bullets represent a variable or a group of variables. Diamonds represent the dependence of the variables linked to it. Corresponding to the  $G$ -by- $E$  matrix of time series, the main parameter structure can be visualized as a matrix, where each row corresponds to a gene-specific parameter  $\phi_g$  and each column corresponds to experiment-specific parameters  $(\mu_e, \psi_e, \lambda_e, \zeta_e)$ . Each cell of the matrix corresponds to the variables specific to a time series. For example, all  $\phi_g$ 's are independent of each other conditional on all  $(\mu_e, \psi_e, \lambda_e, \zeta_e)$ ; a time series is independent of all other time series conditional on the union of  $\phi_g$  and  $(\mu_e, \psi_e, \lambda_e, \zeta_e)$ .*

All variables may be visualized within a gene-by-experiment (i.e.,  $G \times E$ ) matrix (Figure 2), which shows their dependence structure. Each row corresponds to a gene-specific parameter  $\phi_g$  and each column represents the set of experiment-specific parameters  $(\mu_e, \psi_e, \lambda_e, \zeta_e)$ . Each cell of the matrix corresponds to the variables specific to a time series. The gene-specific parameter  $\phi_g$  is the key to integrate the time series for gene  $g$  from multiple experiments. Experiment-specific parameters  $\Theta_e$  are used to pool information across all genes within a particular experiment.

For model comparison, we also introduce the following model ( $M_0$ ) for APE genes:

$$Y_{get} = a_{ge} + b_{ge}T_{et} + c_{ge}(\min(T_{et} - d_{ge}, 0))^2 + \varepsilon_{get}.$$

The only difference between  $M_0$  (null model) and  $M_1$  (alternative model) is the periodic component  $A_{ge} \cos(\mu_e T_{et} + \psi_e + \phi_g) e^{-\lambda_e T_{et}}$ .

**2.3. Identifiability.** In the  $M_1$  model, the phase parameters  $\psi_e$  and  $\phi_g$  are not identifiable because the joint posterior distribution remains the same if we add a constant  $z$  to all  $\psi_e$  and subtract  $z$  from all  $\phi_g$ . This nonidentifiability problem can be solved by fixing one of the phase parameters, but the loss of one degree of freedom makes the MCMC algorithm very “sticky” (slow-mixing). Since we only care about the relative values of  $\psi_e$ 's and  $\phi_g$ 's, we solve the problem by assigning a reasonably tight prior distribution to one of the phase parameters and flatter priors to others, and using a transformation group move to improve mixing of the MCMC chain (see Appendix A.3).

For periodic signal fitting, the angular frequency parameter  $\mu_e$  is usually nonidentifiable because a time series with angular frequency  $\mu_e$  is also a time series with angular frequency  $\mu_e/n$  for any positive integer  $n$ . We avoid this problem by specifying the periodic signal as a damping single sinusoidal curve and limiting the domain of  $\mu_e$  to a bounded range. The bound of  $\mu_e$  is instituted via its prior which is based on our prior knowledge of the cell cycle duration in fission yeast.

*2.4. Bayesian computation.* We estimate all unknown parameters through MCMC simulation of their joint posterior distribution. More specifically, we use a Metropolis-within-Gibbs algorithm to iteratively sample one set of parameters given all the others:

- Step 1: sample experiment-specific parameters  $\Theta_e$  conditional on  $\Phi$ ,  $\Gamma$  and  $Y$ ,
- Step 2: sample gene-specific parameters  $\phi_g$  conditional on  $\Theta$ ,  $\Gamma$  and  $Y$ ,
- Step 3: sample time series-specific parameters  $\Gamma_{ge}$  conditional on  $\Theta$ ,  $\Phi$  and  $Y$ .

The MCMC chain composed of these basic moves suffers from a slow mixing problem caused by strong correlations among some parameters. We can alleviate the problem by parallelizing each of the three steps based on the conditional independence of the parameters. For instance, we can parallelize the sampling of  $\Gamma_{ge}$  from their full conditional distribution since they are independent of each other given  $\Theta$ ,  $\Phi$  and  $Y$ . When some parameters are highly correlated in their joint distribution, single-component moves cause very slow-mixing. To cope with this problem, we designed a new sampler called the Metropolized independence group sampler (MIPS) by combining the ideas of grouping [Liu, Wong and Kong (1994)] and the Metropolized independence sampler [Hastings (1970); Liu (1996); Liu (2001)]. The key idea is to update the whole subset of correlated variables simultaneously independent of the current state using a sequential proposing procedure. MIPS moves are inserted to the main Metropolis-within-Gibbs iteration. The details of the MCMC implementation are given in the [Appendix](#).

*2.5. Strategies for discerning PE genes from APE genes.* We used three statistics to judge which genes are PE ones. Among them, the Bayesian Information Criterion is used to compare the fitting of model  $M_1$  with that of model  $M_0$ , both to real data. The other two statistics measure the periodicity by comparing the fitting of the  $M_1$  model to the real data with that to the permuted data or the data simulated from the  $M_0$  model.

2.5.1. *Permutation test.* Since we fit model  $M_1$  to every gene, even the APE genes are modeled with experiment-specific parameters  $\Theta$  that are primarily determined by PE components. Therefore, to examine the effect of our Bayesian model fitting procedure on APE genes, we generate background data by permuting each time series for every gene in the real data, which destroys any periodic pattern therein. We run the same MCMC algorithm to fit the  $M_1$  model to the background data set by fixing all experiment-specific parameters  $\Theta$  at the posterior mode obtained from the MCMC run for the real data.

2.5.2. *Simulation from the null model.* One problem of using the permutation data as background control is that the permuted time series do not capture the intrinsic autocorrelation of the measured time series, which exists even if it is not periodically expressed. For example, many time series in the real data show a general trend without oscillation, which may be a result of the gene's response to the perturbation caused by synchronization techniques. To accommodate this possible bias, we generate a second data set from the  $M_0$  model. Compared to the permuted time series,  $M_0$  explains the autocorrelation in the time series by a mean curve. We run the same MCMC algorithm to fit  $M_0$  to all genes in the real data.

We simulated from the  $M_0$  model a data set of similar size and structure as the combined real data set. All parameters are simulated from their corresponding prior distributions. Both  $M_1$  and  $M_0$  are fitted to this simulated data set. While fitting  $M_1$ , we fix all experiment-specific parameters  $\Theta$  at the posterior mode obtained from the MCMC run for the real data.

2.5.3. *Model comparison.* One approach for discerning PE genes from APE genes is to use permuted data or data simulated from the null model as background control, and to fit the  $M_1$  model to both the real data and the background data. The fitting of the background data is then used to determine a threshold for the desired false positive rate (FPR). Another approach is to fit both models  $M_1$  and  $M_0$  to the real data, and then do the classification based on a comparison of the fitness of the models. Various information criteria can be used for this task, such as Akaike's Information Criterion (AIC) [Akaike (1973)], the Bayesian Information Criterion (BIC) [Schwarz (1978)] and the Deviance Information Criterion (DIC) [Spiegelhalter et al. (2002)], to just name a few.

A full Bayesian alternative to our approach here is to introduce a latent variable  $I_g$  for each gene to indicate whether it comes from  $M_1$  or  $M_0$ . Then, the reversible-jump strategy [Green (1995)] can be used to build a MCMC sampler to traverse the joint space of the latent indicators and model parameters. But due to the global nature of many parameters in our model, this approach is computationally extremely expensive. Additionally, the results

so obtained may be too sensitive to our model assumptions. Thus, we feel that using randomization and null model approaches in the spirit of posterior predictive model checking [Gelman, Meng and Stern (1996)] provides a more robust detection of PE genes.

2.5.4. *Statistics for periodicity.* We use multiple gene-specific statistics to measure the periodicity of a gene. Based on the fitted parameter values for the  $M_1$  model, we define the gene-specific Signal-to-Noise Ratio ( $SNR$ ) as the relative strength of the fitted periodic component compared to the noise level:

$$SNR_g = \sum_{e=1}^E \frac{\sum_{t=1}^{S_e} \{A_{ge} \cos(\mu_e T_{et} + \psi_e + \phi_g) e^{-\lambda_e T_{et}}\}^2}{\sigma_{ge}^2}.$$

The  $SNR$  statistic combines periodicity information for a gene from every experiment in terms of the amplitude of its periodic component. For each gene, we calculate  $SNR$  for each iteration of the MCMC chain, and then summarize the posterior samples of  $SNR$  using the 2.5th percentile, the 97.5th percentile and the mean. Genes with higher  $SNR$  values are more likely to be periodically expressed. We also use the fitted phase to measure periodicity from the fitted parameters of the  $M_1$  model. More specifically, we use the length of the 95% central posterior interval (denoted by LPI) of a gene's relative phase  $\phi_g + \psi_1$  ( $\psi_1$  is chosen arbitrarily since only the difference of relative phase matters) as one of the periodicity measures. Genes with higher LPIs are less likely to be periodic either because their periodic components are too weak or their multiple time series might show inconsistent peaking time within the cell cycle.

We use the Bayesian Information Criterion difference ( $BIC^{01}$ ) to measure periodicity based on the fitted posterior modes of the two models. Let  $L_g^0$  and  $L_g^1$  denote the likelihood values for gene  $g$  at the posterior mode of the parameters for models  $M_0$  and  $M_1$ , respectively. The model comparison criterion  $BIC^{01}$  is defined as  $BIC_g^{01} = 2 \log(L_g^1) - 2 \log(L_g^0) - (k_1 - k_0) \log(N)$ , where  $N$  is the number of observed data points for the gene, and  $k_0$  and  $k_1$  are the number of free parameters in models  $M_0$  and  $M_1$ , respectively. A gene with positive  $BIC^{01}$  value prefers model  $M_1$  to  $M_0$ . Genes with higher  $BIC^{01}$  values are more likely to be periodically expressed.

### 3. Results and discussion.

3.1. *Model fitting check.* The MCMC chain on the entire real cell cycle data converged in approximately 2000 iterations. The autocorrelation function of the posterior probabilities from each chain showed that the MCMC algorithm is efficient in terms of effective sample sizes after burn-in. The

details of the model fitting diagnosis are given in the supplemental material of this paper [Fan, Pyne and Liu (2009)]. Figure 7 in the supplementary material [Fan, Pyne and Liu (2009)] displays the posterior distribution of the cell cycle length  $2\pi/\mu_e$  for each of the ten experiments. After convergence, the experiment-specific parameters  $\Theta$  showed little variation, that is, their marginal posterior distributions had very small variance compared to their ranges. Based on the posterior mode determined from the MCMC chain, we calculated the residue of each time series. The autocorrelation analysis of the residue showed that by fitting  $M_1$  to the data, the autocorrelation was reduced to the level comparable to those of i.i.d. noise. Comparison of variance reduction between the real and the permuted data suggested that the  $M_1$  model explained a significant amount of variance for most of the genes showing significant autocorrelation in their time series.

*3.2. Number of periodically expressed genes.* We ranked all genes in the order of decreasing posterior mean *SNR* value. Thus, highly ranked genes are more likely to be periodically expressed. We then stratified this sorted list into 6 groups and reordered each group according to the fitted peaking time. Figure 3 shows the whole sorted data set. Strikingly, a periodic pattern stands out for all gene groups after simply reordering them (note that these are simply rearranged original data). The pattern is clear and consistent across all experiments for the top 2000 genes, which suggests that about 40% of all genes in the organism could be periodically expressed. The pattern is still strong for genes in the range 2001–3500. We can even observe periodicity among the remaining genes shown in the bottom group, which, however, is comparable to the top ranking “genes” in the permuted data.

For a comparison with the result from traditional clustering methods, the microarray clustering software Cluster [Eisen et al. (1998)] was used to group genes with similar gene expression. A heatmap similar to Figure 3 is included in the supplemental material of this paper [Fan, Pyne and Liu (2009)]. Compared to the ubiquitous periodic pattern in Figure 3, only several small clusters with visible periodic pattern may be observed from the hierarchical clustering result.

We used two approaches to test whether the visual periodic pattern in Figure 3 is statistically significant. The first approach compares the fitting of the  $M_1$  model to the real and background data, that is, the permuted data or the data simulated from the  $M_0$  model. Two statistics are used to measure the periodicity for this approach. The *SNR* statistic measures the amplitude of the periodic component, while the *LPI* statistic measures the uncertainty of the relative phase of every gene. Figure 4 and Figure 8 in the supplementary material [Fan, Pyne and Liu (2009)] show the estimated posterior densities of these measures. The curves from the background data provide a null distribution for the corresponding statistic, from which we can

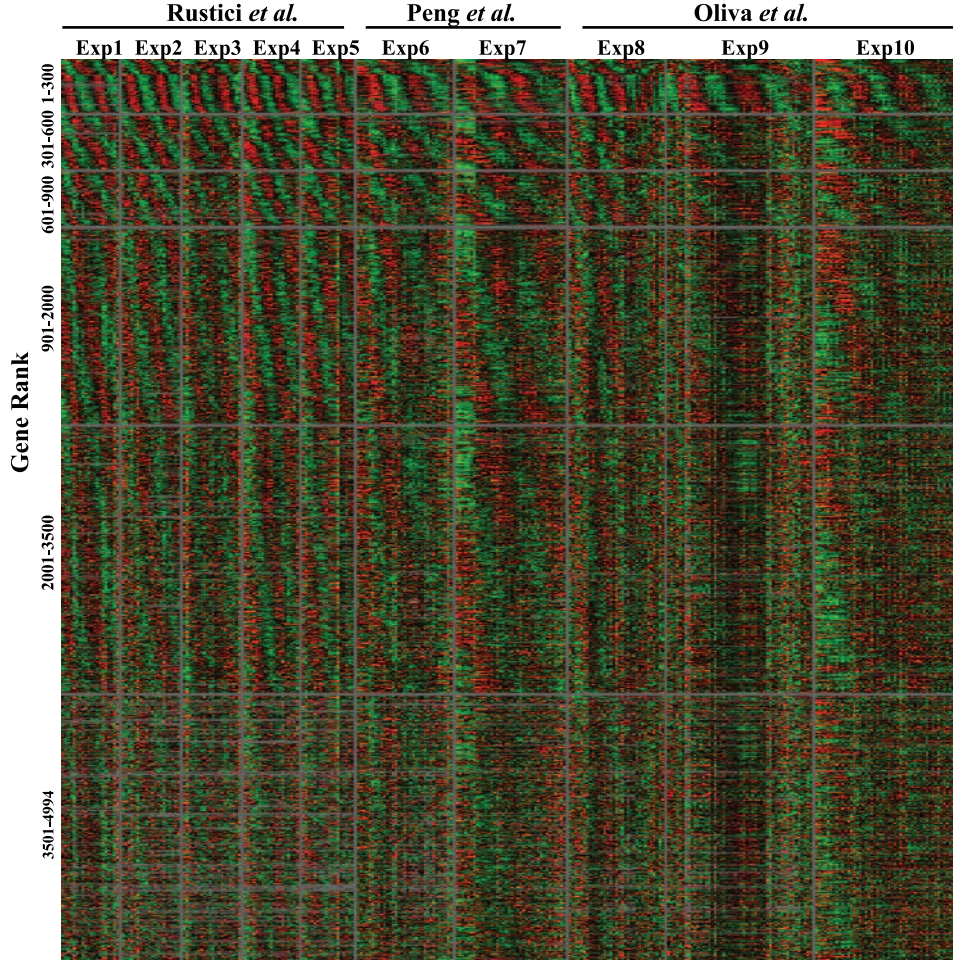


FIG. 3. Heatmap of all genes' time series data ranked by decreasing mean SNR value. Columns correspond to time points, which are grouped by experiment and sorted by time within each group. Rows correspond to genes, which are ranked by their mean SNR value and sorted by their mean peak times within each group. For example, the first row group contains the 300 genes with the highest mean SNR value from our combined analysis of all 10 experiments, and they are sorted by their relative phase  $\phi_g + \psi_1$  within the group. Each time series is normalized to zero mean and unit variance for display. The heatmap is drawn by TreeView [Eisen et al. (1998)] with default setting. Red indicates up-regulation, green indicates down-regulation, black means no change of expression levels, and grey is missing data. It shows a periodic pattern for all gene groups.

estimate FPR for any given threshold. The clear separation of the posterior densities for the real and background data suggests that a lot of genes show a periodic pattern that is stronger than i.i.d. noise or  $M_0$  data. For example, by comparing the LPI curves of the real and permuted data in Figure 8 in the

supplementary material [Fan, Pyne and Liu (2009)], we can claim 3086 PE genes for  $FPR = 0.002$ , corresponding to about 10 false positives. Similarly, by comparing the posterior mean SNR values of the real and permuted data in Figure 4, we can claim 3599 PE genes for  $FPR = 0.002$ . The number of claimed PE genes when using the simulated data from the  $M_0$  model as background control is similar. For instance, the comparison of the posterior mean SNR densities yields 3414 PE genes for  $FPR = 0.002$ , and that of the LPI densities yields 3036 PE genes for  $FPR = 0.002$ .

The second approach compares the fitting of the two models  $M_1$  and  $M_0$ , both using the real data. We used BIC as the model comparison criterion. As shown in Figure 9 in the supplementary material [Fan, Pyne and Liu (2009)], almost all  $BIC^{01}$  values from the permuted data as well as the simulated data from the  $M_0$  model are smaller than zero. For the real data,

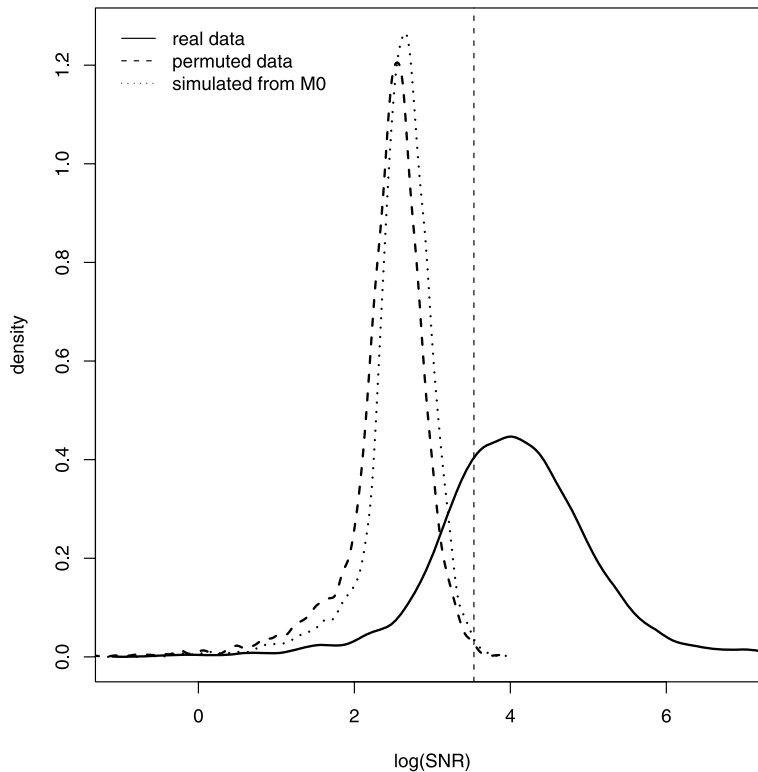


FIG. 4. Density comparison of SNR from the three data sets. The  $M_1$  model is fitted to the real data, permuted data and the data simulated from the  $M_0$  model. For each gene, we get the posterior mean of the SNR statistic from the combined analysis. For each data set, we pool all genes together to get a kernel density estimate, which is shown in this graph. The vertical line indicates the threshold corresponding to  $FPR = 0.002$  in the permuted data, from which one can claim 3599 PE genes from the real data.

TABLE 2  
*Correlation of different statistics and their classification results*

Statistic	SNR	LPI	$BIC^{01}$
SNR	3599	3051	1967
LPI	-0.93	3086	1906
$BIC^{01}$	0.86	-0.83	2003

*Note:* The permuted data was used as background control. The lower-left part of the table shows the Spearman correlation between pairs of statistics. The numbers on the diagonal are the number of PE genes claimed by the corresponding statistic. For SNR, we use a cutoff corresponding to  $FPR = 0.002$  for the two mean SNR density. For LPI, we also use the threshold corresponding to  $FPR = 0.002$ . We use zero as the threshold for  $BIC^{01}$ . The upper-right part of the table shows the number of PE genes claimed by a pair of statistics. Within them, 1898 genes are claimed by all three statistics.

we can claim 2003 PE genes from the combined analysis by using zero as the threshold for  $BIC^{01}$ . Corresponding to this threshold, the permuted data will only produce one false positive PE gene, corresponding to  $FPR = 0.0002$ .

The results of these three statistics are summarized in Table 2. Here we used the permuted data as background control. The average Spearman correlation between pairs of the statistics is 0.87, suggesting that the three statistics are highly consistent in ranking the genes' periodicity. The approaches based on permutation control (SNR, LPI) made more significant claims than the model selection approach. Overall, we obtained a list of 1898 significant PE genes that are claimed by all three statistics.

**3.3. Performance comparison.** To evaluate the performance of identifying PE genes, we defined a benchmark set as the union set of the list of PE genes derived from small-scale experiments [Marguerat et al. (2006)] and a core set of genes whose periodic regulation is conserved between budding yeast and fission yeast [Lu et al. (2007)]. The resulting benchmark set consists of 162 genes. We used this benchmark set to compare our method with the method used by Marguerat et al. (2006).

The statistic used for gene classification by Marguerat et al. (2006) is a score calculated from a  $p$ -value of regulation and a  $p$ -value of periodicity. When combining multiple experiments for gene classification, they multiplied the  $p$ -values from individual experiments to get a total  $p$ -value of regulation and a total  $p$ -value of periodicity. To estimate the FPR of their statistic, we calculated the scores for the permuted data. For our method, we use the SNR statistic for gene classification.

Figure 5 shows the performance of the SNR statistic and Marguerat et al.'s score on both the combined data (all experiments) and the Exp1 data (a single experiment) in the form of ROC curves. For any given FPR value, we

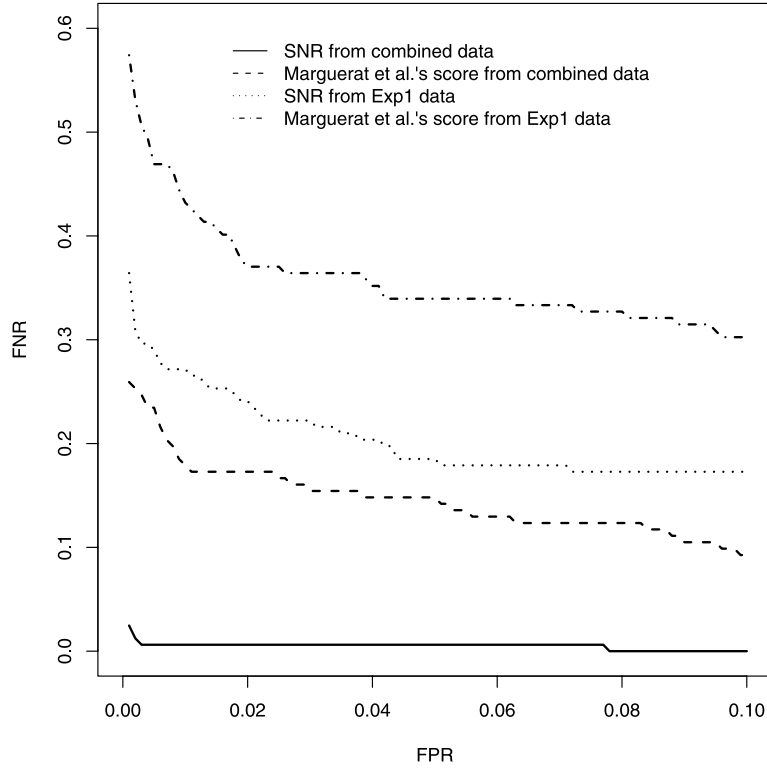


FIG. 5. Performance on the benchmark set. For each of the four methods listed in the figure legend, we plot FNR against FPR under various thresholds. For each threshold, the benchmark set of 162 PE genes is used to estimate FNR. The permuted version of the data is used to estimate FPR. A smaller under-curve area corresponds to a better classification performance for the benchmark set.

estimate the threshold of a statistic from the permuted version of the data. The corresponding false negative rate (FNR) is estimated by the fraction of the genes in the benchmark set that are classified as APE gene according to this threshold. When applied on the data from a single experiment (Exp1 data), the SNR statistic apparently outperforms Marguerat et al.'s score. The gain of statistical power at the single experiment level could be due to our explicit modeling of the trend component and the de-synchronization effect, which makes our model more realistic for the cell cycle time series. When comparing their performances on the combined data, it seems that the SNR statistic increases the statistical power over Marguerat et al.'s score significantly. This is due not only to a more realistic model for single time series, but also to our approach of the Bayesian meta-analysis. Instead of combining the  $p$ -values from individual experiments, we model multiple experiments simultaneously so as to borrow information across experiments.

Figure 5 indicates that the same statistic performed better at discerning PE genes with the combined data than with the data from a single experiment. This is also true when comparing the performances of a statistic using the overall combined versus that using any subset of the experiments. The detailed information is given in Table 2 in the supplementary material [Fan, Pyne and Liu (2009)]. This is natural because any subset contains less information than the full combined data; but on the other hand, it also indicates that each experiment captured some information about genes’ periodicity during the cell cycle.

3.4. *Subset analysis.* To compare three individual studies [Rustici et al. (2004); Oliva et al. (2005); Peng et al. (2005)] and different experimental techniques, we used the same method for the combined data set to fit model  $M_1$  to all three individual data sets, and also the two collections of experiments using different synchronization techniques (elutriation or cdc25 block-release). We first determined the 95% posterior interval of the SNR statistic for each gene to account for the uncertainty of its SNR estimate. Then for comparison of all the subsets at the same significance level, we claim a gene to be PE if its posterior mean SNR value is above the upper 97.5% posterior limits of the SNR of at least 4984 (out of 4994) permuted “genes.” For the combined data, we thus claimed 2032 PE genes. Figure 6(a) and Figure 6(b) show the overlap of the results from our subset analyses. Figure 6(c) shows the overlap of the original results from the three individual studies. There are 976 genes which are reported as PE by our combined analysis but not by any of the three original studies. Supporting evidences for these genes are included in the supplementary material [Fan, Pyne and Liu (2009)].

Similar to Figure 6(c), the discrepancy about the count and identity of PE genes exists between individual data sets [Figure 6(a)] and across synchronization techniques [Figure 6(b)] although we have unified the whole analysis procedure. Therefore, instead of attributing the discrepancy between the subsets to inconsistent gene naming or use of different analysis methods or arbitrary thresholds [Marguerat et al. (2006)], we suggest that the cause is intrinsic to the data. It also shows that most genes in the discrepant part show significant periodicity in the combined analysis. The combined analysis also captured many genes which can not be detected by subset data analysis. Combined with the benchmark analysis, we observed that 5 out of the 40 benchmark genes whose periodicity have been confirmed by small-scale experiments [Marguerat et al. (2006)] were missed by all three original studies as well as our combined analysis. On the other hand, 6 out of the 92 core environmental stress response genes with known function [Chen et al. (2003)] were claimed as periodically expressed by all three original studies as well as by our combined analysis, suggesting that their periodic signal

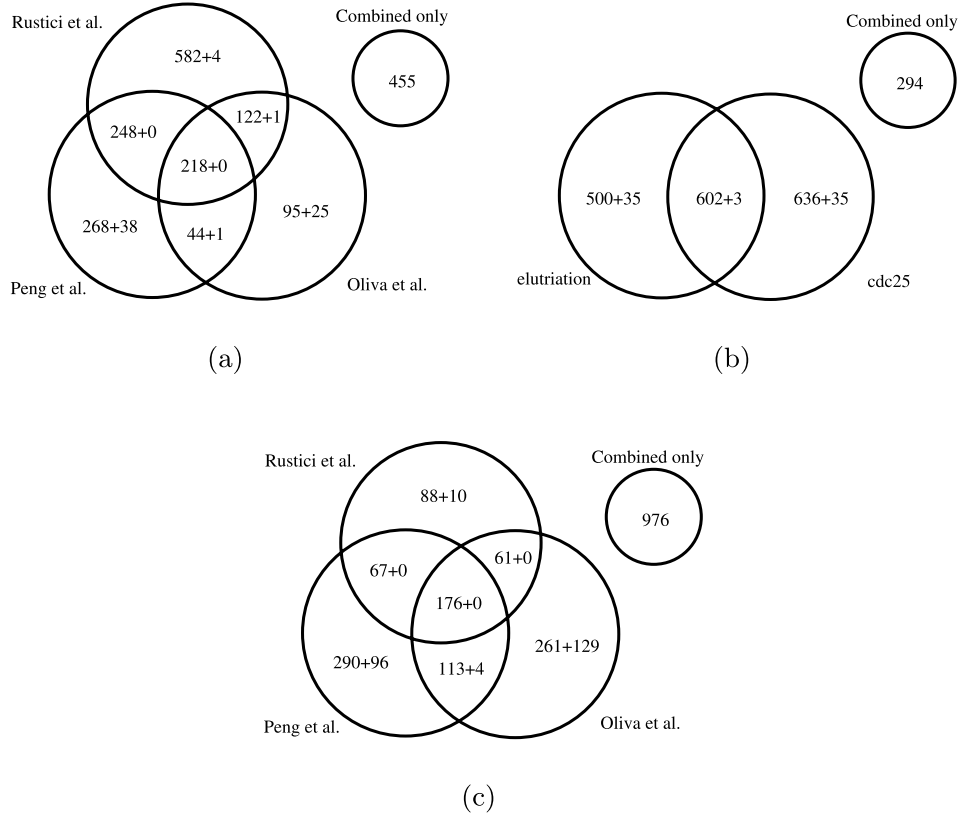


FIG. 6. Venn diagrams showing overlap between claimed PE genes from subsets of the data. Each gene set in all diagrams is compared with the result from the combined analysis that we did using our method. The number before the plus sign is the number of genes also claimed as periodically expressed by our combined analysis. The stand-alone circle represents the part which is reported only by the combined analysis. (a) Comparing the results from individual data sets using our method. (b) Comparing the results from two synchronization techniques using our method. (c) Comparing the results reported in original studies.

is clear to all methods. Possibly, the periodicity measure for widely used positive or negative benchmark sets are not quite accurate.

To investigate the discrepancy between different subsets, we systematically tested these subsets' pairwise reproducibility using the posterior mean SNR values. If it is true that the genes have an intrinsic order in terms of periodicity and all individual data sets are of similar quality in revealing this ordering information, the periodicity measures across pairs of subsets should be consistent. Each data set yields a SNR vector measuring the periodicity of all genes. The key idea is to check whether the Spearman correlation of the two SNR vectors is still significant after removing genes which are top

ranked in both vectors. The details are shown in Figure 10 in the supplementary material [Fan, Pyne and Liu (2009)]. After removing the 847 genes that are highly ranked by both Peng et al. and Oliva et al., the remaining genes' SNR values from these two data sets show no positive Spearman correlation at the significance level of 0.05. This sets the number of reproducible genes supported by these two data sets (5 experiments) to 847. This same count increases to 934 for Rustici et al. versus Peng et al. (7 experiments), and to 1008 for Rustici et al. versus Oliva et al. (8 experiments). The increasing of reproducible genes is consistent with the increase in the size of data involved in comparison. The number further increases to 1554 when comparing elutriation experiments with *cdc25* experiments. This suggests that although the number of reproducible genes is less than the number of PE genes suggested by the combined analysis, the reproducibility is improved by including more data in the comparison or by partitioning the data according to the experiment technique.

To explain the above subset discrepancy, possible flaws in the benchmark sets and the high number of significant genes in the combined analysis, we hypothesize a network-based dynamics for the cell cycle process. For instance, periodic signals from transcription of key cell cycle-regulated genes propagate through the relevant downstream regulatory networks of the organism potentially targeting a considerable number of genes. Thus, depending on the status of the network, these genes may show an observable periodic pattern under one condition, and be too weak to detect under another condition. As a consequence of the combined effect of the variation in periodicity and experimental noise, each study could capture a different subset of the PE genes. The difference of the cell cycle length shown in Figure 7 in the supplementary material [Fan, Pyne and Liu (2009)], which could not be explained solely by microarray platform difference, is a further evidence of such variation. For example, the cell cycle lengths in the posterior mode for the two *cdc25* experiments in Rustici et al. are 135 and 138 minutes, while in Oliva et al. and Peng et al., this number increases to 164 and 173 minutes, respectively. Although they are using the same synchronization technique on the same organism, subtle environmental or physiological differences have changed the speed of the cell cycle oscillation. Therefore, it may have also changed relative amplitudes of oscillation of the genes leading to overall ranking discrepancy.

**4. Conclusion.** In spite of the rapid rise in the number of microarray experiments, many of which address related issues, a systematic meta-analysis of such data is rarely attempted. We conducted a meta-analysis of ten fission yeast cell cycle genome-wide time-series experiments with a model-based Bayesian approach. Compared to other methods, key features of our model include the fixed relative phase of the peaking time of the genes across all

experiments (e.g., a gene will peak 10 degrees earlier than another gene in an experiment if and only if the same happens in another experiment) and a flexible amplitude for periodic components. Our approach does not require training sets to estimate important global parameters such as the period of cell cycle, but to infer them from all the data. Notably, our parametric approach deals with phase shift, signal amplitude difference, noise level difference and de-synchronization automatically. Despite the high dimensionality, the implemented MCMC chain mixes well with the help of global moves. The residual analysis shows that our model fits the data well.

A striking finding of our analysis is that more than 2000 genes are significantly periodically expressed, which accounts for approximately 40% of all the genes in the fission yeast genome. The subset analysis suggests that this number may increase with more data included. This enhances greatly the current knowledge of only 10–15% of all fission yeast genes that are reported as periodically expressed during the cell cycle. Interestingly, genome-wide oscillation has also been reported by recent studies on other cyclic phenomena in the cell, such as the metabolic cycle and circadian periodicity [Klavec et al. (2004); Tu et al. (2005); Ptitsyn, Zvonik and Gimble (2007)]. Clearly, a certain amount of influence of the global cell cycle processes on most genes in the genome, in particular, in unicellular organisms such as fission yeast, cannot be ruled out. For instance, the folding and unfolding of chromosomes over the course of the cell cycle will have genome-wide incidental effect on transcription. However, earlier studies concede that limited ability to distinguish precisely the weakly periodic oscillations from prevalent microarray noise only allowed conservative estimates of PE genes. By explicitly modeling periodic and nonperiodic components, and different sources of variation and noise, our model-based approach helps to overcome this long-standing limitation. The resulting list of more than 2000 PE genes would allow the researchers to cast a much wider and deeper net for cell cycle regulated genes that can lead to investigation of novel or relatively less known gene modules and networks involved in the machinery of cell cycle regulation.

It should be noted that the key idea behind our model is rather general. It can be applied to detect periodic patterns where the amplitude is noisy but the patterns are nonetheless consistent across different experiments. The data can be any collection of time series. A study of cell cycle data from other species, such as the budding yeast, mouse, human, etc., using the proposed method can be of immediate interest.

One possible way to improve the current method is to employ a more robust error model, using, for example,  $t$ -distributions instead of Gaussians for the noise term [Hampel et al. (1986); Lange, Little and Taylor (1989)]. But as a price to pay, the computational complexity may be increased substantially. It should be noted that, as stated in Section 2.5.3, alternative Bayesian model selection methods may also be applied to this problem. For

example, Green (1995) provides a way to perform joint model selection and parameter estimation via reversible jump MCMC. It may be applicable to this problem if the efficiency of reversible jump MCMC moves can be improved significantly. The methods proposed by Chib (1995) and Chib and Jeliazkov (2001), which estimate the marginal likelihood of the data under a model, may also be a worthwhile direction to explore.

## APPENDIX: MCMC IMPLEMENTATION

**A.1. Prior distribution.** We assigned reasonably diffuse but still proper prior distributions for all parameters:

$$\begin{aligned}
 a_{ge} &\sim N(0, C_1), \\
 b_{ge} &\sim N(0, C_2), \\
 c_{ge} &\sim N(0, C_3), \\
 d_{ge} &\sim \text{Unif}(0, C_4), \\
 A_{ge} &\propto \text{Exp}(\text{rate} = C_5), \quad 0 \leq A_{ge} < C_6, \\
 \mu_e &\sim \text{Unif}(C_7, C_8), \\
 \psi_1 &\propto N(0, C_9), \quad -\pi \leq \psi_1 < \pi, \\
 \psi_e &\propto N(0, C_{10}), \quad e = 2, \dots, E, -\pi \leq \psi_e < \pi, \\
 \phi_g &\sim \text{Unif}(-\pi, \pi), \\
 \lambda_e &\sim \text{Unif}(0, C_{11}), \\
 \sigma_{ge}^2 | \zeta_e &\sim \text{Inv-}\chi^2(C_{12}, \zeta_e), \\
 \zeta_e &\sim \text{Exp}(C_{13}).
 \end{aligned}$$

The constants in the prior distributions are assigned correspondingly, making use of our prior knowledge:  $C_1 = 1, C_2 = 0.005^2, C_3 = 0.0001^2, C_4 = 500, C_5 = 10, C_6 = 10, C_7 = 2\pi/180, C_8 = 2\pi/120, C_9 = 0.2^2, C_{10} = 1^2, C_{11} = 0.006, C_{12} = 4, C_{13} = 50$ .

**A.2. Posterior distributions and Metropolis-within-Gibbs.** We can write down the joint distribution of the data and parameters as

$$\begin{aligned}
 &p(Y, \Theta, \Phi, \Gamma) \\
 &= p(Y|\Theta, \Phi, \Gamma)p(\Theta, \Phi, \Gamma) \\
 &= \left[ \prod_{g=1}^G \left\{ \prod_{e=1}^E \left\langle \prod_{t=1}^{S_e} p(Y_{get} | a_{ge}, b_{ge}, c_{ge}, d_{ge}, A_{ge}, \sigma_{ge}^2, \phi_g, \mu_e, \psi_e, \lambda_e) \right\rangle \right\} \right]
 \end{aligned}$$

$$\begin{aligned} & \left. \begin{aligned} & \times p(a_{ge})p(b_{ge})p(c_{ge})p(d_{ge})p(A_{ge})p(\sigma_{ge}^2|\zeta_e) \end{aligned} \right\} \\ & \left. \begin{aligned} & \times p(\phi_g) \end{aligned} \right] \\ & \times \left\langle \prod_{e=1}^E p(\mu_e)p(\psi_e)p(\lambda_e)p(\zeta_e) \right\rangle. \end{aligned}$$

We assume that all missing data are missing completely at random, so their corresponding components are simply omitted from this expression.

Again, we introduce the following symbols for convenience:

$$\begin{aligned} D_{get} &\equiv Y_{get} - a_{ge} - b_{ge}T_{et} - c_{ge}(\min(T_{et} - d_{ge}, 0))^2, \\ R_{get} &\equiv D_{get} - A_{ge} \cos(\mu_e T_{et} + \psi_e + \phi_g) e^{-\lambda_e T_{et}}, \\ X_{get} &\equiv (1, T_{et}, [\min(T_{et} - d_{ge}, 0)]), \\ X_{ge} &\equiv \begin{pmatrix} X_{ge1} \\ \vdots \\ X_{geS_e} \end{pmatrix}, \\ Z_{get} &\equiv Y_{get} - A_{ge} \cos(\mu_e T_{et} + \psi_e + \phi_g) e^{-\lambda_e T_{et}}, \\ Z_{ge} &\equiv \begin{pmatrix} Z_{ge1} \\ \vdots \\ Z_{geS_e} \end{pmatrix}, \\ V &\equiv \begin{bmatrix} \frac{1}{C_1} & & \\ & \frac{1}{C_2} & \\ & & \frac{1}{C_3} \end{bmatrix}. \end{aligned}$$

From the joint distribution, we can get all full conditional posterior distributions:

$$\begin{aligned} \begin{pmatrix} a_{ge} \\ b_{ge} \\ c_{ge} \end{pmatrix} \Big|_{rest} &\sim N\left(\left(\frac{X_{ge}^T X_{ge}}{\sigma_{ge}^2} + V\right)^{-1} \frac{X_{ge}^T Z_{ge}}{\sigma_{ge}^2}, \left(\frac{X_{ge}^T X_{ge}}{\sigma_{ge}^2} + V\right)^{-1}\right), \\ p(d_{ge}|rest) &\propto \frac{1}{C_4} \exp\left\{-\frac{\sum_{t=1}^{S_e} R_{get}^2}{2\sigma_{ge}^2}\right\}, \\ A_{ge}|rest &\propto N(\mu, \sigma^2), \quad 0 \leq A_{ge} < C_6, \end{aligned}$$

where

$$\mu = \frac{\sum_{t=1}^{S_e} \cos(\mu_e T_{et} + \psi_e + \phi_g) e^{-\lambda_e T_{et}} D_{get} - \sigma_{ge}^2 C_5}{\sum_{t=1}^{S_e} \{\cos(\mu_e T_{et} + \psi_e + \phi_g) e^{-\lambda_e T_{et}}\}^2},$$

$$\sigma^2 = \frac{\sigma_{ge}^2}{\sum_{t=1}^{S_e} \{\cos(\mu_e T_{et} + \psi_e + \phi_g) e^{-\lambda_e T_{et}}\}^2},$$

$$p(\mu_e | rest) \propto \frac{1}{C_8 - C_7} \prod_{g=1}^G \prod_{t=1}^{S_e} \exp\left\{-\frac{R_{get}^2}{2\sigma_{ge}^2}\right\}, \quad C_7 \leq \mu_e < C_8,$$

$$p(\psi_e | rest) \propto C_9^{-0.5} \prod_{g=1}^G \prod_{t=1}^{S_e} \exp\left\{-\frac{R_{get}^2}{2\sigma_{ge}^2} - \frac{\psi_e^2}{2C_9}\right\}, \quad -\pi \leq \psi_e < \pi, \text{ for } e = 1,$$

$$p(\psi_e | rest) \propto C_{10}^{-0.5} \prod_{g=1}^G \prod_{t=1}^{S_e} \exp\left\{-\frac{R_{get}^2}{2\sigma_{ge}^2} - \frac{\psi_e^2}{2C_{10}}\right\},$$

$-\pi \leq \psi_e < \pi, \text{ for } e = 2, \dots, E,$

$$p(\phi_g | rest) \propto \prod_{g=1}^G \prod_{t=1}^{S_e} \exp\left\{-\frac{R_{get}^2}{2\sigma_{ge}^2}\right\}, \quad -\pi \leq \phi_g < \pi,$$

$$p(\lambda_e | rest) \propto \prod_{g=1}^G \prod_{t=1}^{S_e} \exp\left\{-\frac{R_{get}^2}{2\sigma_{ge}^2}\right\}, \quad 0 \leq \lambda_e < C_{11},$$

$$\sigma_{ge}^2 \sim \text{Inv-}\chi^2\left(S_e + C_{12}, \frac{C_{12}\zeta_e + \sum_{t=1}^{S_e} R_{get}^2}{S_e + C_{12}}\right),$$

$$\zeta_e \sim \text{Gamma}\left(\frac{C_{12}}{2}G + 1, \frac{C_{12}}{2} \sum_{g=1}^G \frac{1}{\sigma_{ge}^2} + C_{13}\right).$$

For conditional distributions which we only know up to a normalization constant, we used the Metropolis–Hastings algorithm to draw samples. When fitting the  $M_0$  model to a gene, the full conditional distribution of its parameters can be obtained by simply replacing all  $A_{ge}$  with zero in the corresponding full conditional distribution from  $M_1$ .

**A.3. Advanced MCMC moves for better mixing.** Besides the basic Metropolis-within-Gibbs iteration, we insert the following moves to perturb the MCMC chain in order to help it traverse faster through the high dimensional space where there are many local modes and strong correlations among a group of parameters.

- Phase parameters  $\psi_e$  and  $\phi_g$  are not identifiable in model  $M_1$  because the joint posterior distribution is invariant if we add a value to all  $\psi_e$  and subtract the same value from all  $\phi_g$ . One way to solve this nonidentifiability problem is to fix one of them, but it appears that the loss of one degree of freedom makes the chain very sticky, that is, slow to converge. As an alternative, we assign zero-centered normal prior distributions to all  $\psi_e$ , and use a transformation group move [Liu and Wu (1999); Liu and Sabatti (2000); Liu (2001)] to improve mixing of the MCMC sampler. Specifically, we first propose a move by adding a random number  $z$  to all  $\psi_e$  and subtracting  $z$  from all  $\phi_g$ , and then use the Metropolis–Hastings rule to accept or reject this move. Since we only care about the relative phases of genes and experiments, we use  $\phi_g + \psi_1$  as the gene’s relative phase and  $\psi_e - \psi_1$  as the phase for an experiment.
- When a gene violates the assumption that its peaking time in the cell cycle relative to all other genes is fixed across different experiments, its multiple time series will show inconsistent phases, which leads to multiple modes for its phase parameter  $\phi_g$  and amplitude parameters  $A_{ge}$ . It is difficult to get out of this kind of local mode by updating  $\phi_g$  and  $A_{ge}$  separately and locally. We combine the idea of grouping [Liu, Wong and Kong (1994)] and Metropolized independence sampling [Hastings (1970); Liu (1996, 2001)] to deal with this kind of local mode. We call it the Metropolized independence group sampler (MIPS). We first propose a new  $\phi_g$  independent of old  $\phi_g$ , say, from its prior distribution or an approximation of its conditional posterior distribution. Then, we sample all  $A_{ge}$  conditional on the new  $\phi_g$ . The Metropolis–Hastings rule is used to decide whether to accept this move or not. To get a good proposal of  $A_{ge}$ , we use linear regression to get the least square estimate of  $A_{ge}$  and use it as the center of the proposal distribution of  $A_{ge}$ .
- We again use MIPS to deal with the strong correlation within the trend parameters  $(a_{ge}, b_{ge}, c_{ge}, d_{ge})$  for a time series. The key is to propose a new  $d_{ge}$  independent of the old  $d_{ge}$  and sample  $(a_{ge}, b_{ge}, c_{ge})$  jointly conditional on the new  $d_{ge}$ , which is a multivariate normal distribution here.
- There are also strong correlations between  $\lambda_e$  and all  $A_{ge}$  of the same experiment  $e$ . We still use MIPS to perturb the MCMC chain. We propose a new  $\lambda_e$  independent of the old  $\lambda_e$  and sample all  $A_{ge}$  of the same experiment  $e$  conditional on the new  $\lambda_e$ . Similar to the MIPS moves for  $\phi_g$  and  $A_{ge}$  of the same gene  $g$ , we used the least square estimate of  $A_{ge}$  to improve the proposal efficiency.

It should be noted that MIPS improves the mixing of the MCMC chain, especially at the initial state of the sampling, with an extra cost in computation. Our simulations indicated that this is a worthy effort. In meta-analysis, it is not unusual that different experiments support different values

for a shared parameter. As a result, the shared parameter may have a multimodal distribution. In that case, strategies such as MIPS for making global moves are desirable.

**Acknowledgments.** We thank Professor Xiao-Li Meng for his helpful suggestions that led to a modification of the model in this paper. We are also grateful to Professor Wing H. Wong and Dr. Xin Lu for their valuable comments. All R codes and fitting results are available upon request.

### SUPPLEMENTARY MATERIAL

**Various supporting materials** (DOI: [10.1214/09-AOAS300SUPP](https://doi.org/10.1214/09-AOAS300SUPP); .pdf). In this supplement we provide model fitting diagnoses, hierarchical clustering results, the effect of data size on the statistical power, supporting evidences for newly found genes, and figures referred to in this paper.

### REFERENCES

- AHDESMAKI, M., LAHDESMAKI, H., PEARSON, R., HUTTUNEN, H. and YLI-HARJA, O. (2005). Robust detection of periodic time series measured from biological systems. *BMC Bioinformatics* **6** 117.
- AKAIKE, H. (1973). Information theory and an extension of the maximum likelihood principle. In *Second International Symposium on Information Theory* (B. N. Petrox and F. Caski, eds.) 267–281. Akademiai Kiado, Budapest. [MR0483125](#)
- BAR-JOSEPH, Z., SIEGFRIED, Z., BRANDEIS, M., BRORS, B., LU, Y., EILS, R., DYNLACHT, B. D. and SIMON, I. (2008). Genome-wide transcriptional analysis of the human cell cycle identifies genes differentially regulated in normal and cancer cells. *Proc. Natl. Acad. Sci. USA* **105** 956–961.
- CHEN, D., TOONE, W. M., MATA, J., LYNE, R., BURNS, G., KIVINEN, K., BRAZMA, A., JONES, N. and BAHLER, J. (2003). Global transcriptional responses of fission yeast to environmental stress. *Mol. Biol. Cell* **14** 214–229.
- CHIB, S. (1995). Marginal likelihood from the Gibbs output. *J. Amer. Statist. Assoc.* **90** 1313–1321. [MR1379473](#)
- CHIB, S. and JELIAZKOV, I. (2001). Marginal likelihood from the metropolis hastings output. *J. Amer. Statist. Assoc.* **96** 270–281. [MR1952737](#)
- CHO, R. J., CAMPBELL, M. J., WINZELER, E. A., STEINMETZ, L., CONWAY, A., WODICKA, L., WOLFSBERG, T. G., GABRIELIAN, A. E., LANDSMAN, D., LOCKHART, D. J. and DAVIS, R. W. (1998). A genome-wide transcriptional analysis of the mitotic cell cycle. *Mol. Cell* **2** 65–73.
- DE LICHTENBERG, U., JENSEN, L. J., FAUSBOLL, A., JENSEN, T. S., BORK, P. and BRUNAK, S. (2005). Comparison of computational methods for the identification of cell cycle-regulated genes. *Bioinformatics* **21** 1164–1171.
- EISEN, M. B., SPELLMAN, P. T., BROWN, P. O. and BOTSTEIN, D. (1998). Cluster analysis and display of genome-wide expression patterns. *Proc. Natl. Acad. Sci. USA* **95** 14863–14868.
- FAN, X., PYNE, S. and LIU, J. S. (2009). Supplement to “Bayesian meta-analysis for identifying periodically expressed genes in fission yeast cell cycle.” DOI: [10.1214/09-AOAS300SUPP](https://doi.org/10.1214/09-AOAS300SUPP).

- FUTSCHIK, M. E. and HERZEL, H. (2008). Are we overestimating the number of cell-cycling genes? The impact of background models on time-series analysis. *Bioinformatics* **24** 1063–1069.
- GELMAN, A., MENG, X.-L. and STERN, H. (1996). Posterior predictive assessment of model fitness via realized discrepancies. *Statist. Sinica* **6** 733–807. [MR1422404](#)
- GREEN, P. J. (1995). Reversible jump Markov chain Monte Carlo computation and Bayesian model determination. *Biometrika* **82** 711–732. [MR1380810](#)
- HAMPEL, F. R., RONCHETTI, E. M., ROUSSEEUW, P. J. and STAHEL, W. A. (1986). *Robust Statistics: The Approach Based on Influence Functions*. Wiley, New York. [MR0829458](#)
- HASTINGS, W. K. (1970). Monte Carlo sampling methods using Markov chains and their applications. *Biometrika* **57** 97–109.
- HERTZ-FOWLER, C., PEACOCK, C. S., WOOD, V., ASLETT, M., KERHORNOU, A., MOONEY, P., TIVEY, A., BERRIMAN, M., HALL, N., RUTHERFORD, K., PARKHILL, J., IVENS, A. C., RAJANDREAM, M.-A. and BARRELL, B. (2004). GeneDB: A resource for prokaryotic and eukaryotic organisms. *Nucl. Acids Res.* **32** (Suppl 1) D339–D343.
- ISHIDA, S., HUANG, E., ZUZAN, H., SPANG, R., LEONE, G., WEST, M. and NEVINS, J. R. (2001). Role for E2F in control of both DNA replication and mitotic functions as revealed from DNA microarray analysis. *Mol. Cell. Biol.* **21** 4684–4699.
- JOHANSSON, D., LINDGREN, P. and BERGLUND, A. (2003). A multivariate approach applied to microarray data for identification of genes with cell cycle-coupled transcription. *Bioinformatics* **19** 467–473.
- KLEVECZ, R. R., BOLEN, J., FORREST, G. and MURRAY, D. B. (2004). From the cover: A genomewide oscillation in transcription gates DNA replication and cell cycle. *Proc. Natl. Acad. Sci. USA* **101** 1200–1205.
- LANGE, K. L., LITTLE, R. J. A. and TAYLOR, J. M. G. (1989). Robust statistical modeling using the t distribution. *J. Amer. Statist. Assoc.* **84** 881–896. [MR1134486](#)
- LAUB, M. T., MCADAMS, H. H., FELDBLYUM, T., FRASER, C. M. and SHAPIRO, L. (2000). Global analysis of the genetic network controlling a bacterial cell cycle. *Science* **290** 2144–2148.
- LIU, D., UMBACH, D. M., PEDDADA, S. D., LI, L., CROCKETT, P. W. and WEINBERG, C. R. (2004). A random-periods model for expression of cell-cycle genes. *Proc. Natl. Acad. Sci. USA* **101** 7240–7245.
- LIU, J. S. (1996). Metropolized independent sampling with comparisons to rejection sampling and importance sampling. *Statist. Comput.* **6** 113–119.
- LIU, J. S. (2001). *Monte Carlo Strategies in Scientific Computing*. Springer, New York. [MR1842342](#)
- LIU, J. S. and SABATTI, C. (2000). Generalised Gibbs sampler and multigrid Monte Carlo for Bayesian computation. *Biometrika* **87** 353–369. [MR1782484](#)
- LIU, J. S., WONG, W. H. and KONG, A. (1994). Covariance structure of the Gibbs sampler with applications to the comparisons of estimators and augmentation schemes. *Biometrika* **81** 27–40. [MR1279653](#)
- LIU, J. S. and WU, Y. N. (1999). Parameter expansion for data augmentation. *J. Amer. Statist. Assoc.* **94** 1264–1274. [MR1731488](#)
- LU, X., ZHANG, W., QIN, Z. S., KWAST, K. E. and LIU, J. S. (2004). Statistical resynchronization and Bayesian detection of periodically expressed genes. *Nucl. Acids Res.* **32** 447–455.
- LU, Y., MAHONY, S., BENOS, P., ROSENFELD, R., SIMON, I., BREEDEN, L. and BAR-JOSEPH, Z. (2007). Combined analysis reveals a core set of cycling genes. *Genome Biology* **8** R146.

- LUAN, Y. and LI, H. (2004). Model-based methods for identifying periodically expressed genes based on time course microarray gene expression data. *Bioinformatics* **20** 332–339.
- MARGUERAT, S., JENSEN, T. S., DE LICHTENBERG, U., WILHELM, B. T., JENSEN, L. J. and BAHLER, J. (2006). The more the merrier: Comparative analysis of microarray studies on cell cycle-regulated genes in fission yeast. *Yeast* **23** 261–277.
- MENGES, M., HENNIG, L., GRUISSEM, W. and MURRAY, J. A. (2002). Cell cycleregulated gene expression in arabidopsis. *J. Biol. Chem.* **277** 41987–42002.
- OLIVA, A., ROSEBROCK, A., FERREZUELO, F., PYNE, S., CHEN, H., SKIENA, S., FUTCHER, B. and LEATHERWOOD, J. (2005). The cell cycle-regulated genes of *Schizosaccharomyces pombe*. *PLoS Biology* **3** e225.
- PENG, X., KARUTURI, R. K. M., MILLER, L. D., LIN, K., JIA, Y., KONDU, P., WANG, L., WONG, L.-S., LIU, E. T., BALASUBRAMANIAN, M. K. and LIU, J. (2005). Identification of cell cycle-regulated genes in fission yeast. *Mol. Biol. Cell* **16** 1026–1042.
- PTITSYN, A. A., ZVONIC, S. and GIMBLE, J. M. (2007). Digital signal processing reveals circadian baseline oscillation in majority of mammalian genes. *PLoS Computational Biology* **3** e120. [MR2367257](#)
- RUSTICI, G., MATA, J., KIVINEN, K., LIO, P., PENKETT, C. J., BURNS, G., HAYLES, J., BRAZMA, A., NURSE, P. and BAHLER, J. (2004). Periodic gene expression program of the fission yeast cell cycle. *Nature Genetics* **36** 809–817.
- SCHWARZ, G. (1978). Estimating the dimension of a model. *Ann. Statist.* **6** 461–464. [MR0468014](#)
- SHEDDEN, K. and COOPER, S. (2002). Analysis of cell-cycle-specific gene expression in human cells as determined by microarrays and double-thymidine block synchronization. *Proc. Natl. Acad. Sci. USA* **99** 4379–4384.
- SHERR, C. J. (1996). Cancer cell cycles. *Science* **274** 1672–1677.
- SPELLMAN, P. T., SHERLOCK, G., ZHANG, M. Q., IYER, V. R., ANDERS, K., EISEN, M. B., BROWN, P. O., BOTSTEIN, D. and FUTCHER, B. (1998). Comprehensive identification of cell cycle-regulated genes of the yeast *saccharomyces cerevisiae* by microarray hybridization. *Mol. Biol. Cell* **9** 3273–3297.
- SPIEGELHALTER, D., BEST, N., CARLIN, B. and VAN DER LINDE, A. (2002). Bayesian measures of model complexity and fit. *J. Roy. Statist. Soc. Ser. B* **64** 583–616. [MR1979380](#)
- TSIPORKOVA, E. and BOEVA, V. (2008). Fusing time series expression data through hybrid aggregation and hierarchical merge. *Bioinformatics* **24** i63–i69.
- TU, B. P., KUDLICKI, A., ROWICKA, M. and MCKNIGHT, S. L. (2005). Logic of the yeast metabolic cycle: Temporal compartmentalization of cellular processes. *Science* **310** 1152–1158.
- WHITFIELD, M. L., SHERLOCK, G., SALDANHA, A. J., MURRAY, J. I., BALL, C. A., ALEXANDER, K. E., MATESE, J. C., PEROU, C. M., HURT, M. M., BROWN, P. O. and BOTSTEIN, D. (2002). Identification of genes periodically expressed in the human cell cycle and their expression in tumors. *Mol. Biol. Cell* **13** 1977–2000.
- WICHERT, S., FOKIANOS, K. and STRIMMER, K. (2004). Identifying periodically expressed transcripts in microarray time series data. *Bioinformatics* **20** 5–20.
- WILLBRAND, K., RADVANYI, F., NADAL, J.-P., THIERY, J.-P. and FINK, T. M. A. (2005). Identifying genes from up-down properties of microarray expression series. *Bioinformatics* **21** 3859–3864.
- ZHAO, L. P., PRENTICE, R. and BREEDEN, L. (2001). Statistical modeling of large microarray data sets to identify stimulus-response profiles. *Proc. Natl. Acad. Sci. USA* **98** 5631–5636.
- ZHOU, C., WAKEFIELD, J. and BREEDEN, L. (2005). Bayesian analysis of cell-cycle gene expression data. UW Biostatistics Working Paper Series, Working Paper 276.

X. FAN  
DEPARTMENT OF STATISTICS  
HARVARD UNIVERSITY  
ONE OXFORD STREET  
CAMBRIDGE, MASSACHUSETTS 02138  
USA

AND  
DEPARTMENT OF STATISTICS  
CHINESE UNIVERSITY OF HONG KONG  
SHATIN, N.T.  
HONG KONG  
E-MAIL: [xfan@stat.harvard.edu](mailto:xfan@stat.harvard.edu)  
[xfan@sta.cuhk.edu.hk](mailto:xfan@sta.cuhk.edu.hk)

S. PYNE  
BROAD INSTITUTE OF MIT AND HARVARD  
7 CAMBRIDGE CENTER  
CAMBRIDGE, MASSACHUSETTS 02142  
USA  
E-MAIL: [spyne@broad.mit.edu](mailto:spyne@broad.mit.edu)

J. S. LIU  
DEPARTMENT OF STATISTICS  
HARVARD UNIVERSITY  
ONE OXFORD STREET  
CAMBRIDGE, MASSACHUSETTS 02138  
USA  
E-MAIL: [jliu@stat.harvard.edu](mailto:jliu@stat.harvard.edu)